Stable Equilibrium of a Mechanical Energy Storage Device

Steven Odi-Owei, Kenny Ayoka

Department of Mechanical Engineering, Faculty of Engineering, Rivers State University, Port Harcourt, Nigeria

Email address:

steveodiowei252@gmail.com (Steven Odi-Owei)

Abstract: This study determines the energy of a fatigue-loaded shaft of circular cross-section, in stable equilibrium, deflecting during rotation even in the absence of external loads. The shaft is subjected to completely reversed stresses as well as torsion and bending stresses varying with rotation and introducing fatigue loading problems. The research was conducted in order to establish equilibrium condition at which a shaft subjected to fatigue loading can operate without axial vibration problems, divergence buckling, and instability at critical or above critical speeds. When inertia slows the shaft to rest, where the energy goes usually causes the shaft to rattle. At rest, kinetic energy is zero at that point while potential energy is maximum. The stability status of the shaft can eliminate rattling. The energy method is used, in this study, to develop force-displacement relations. It is also used to show that the total potential energy is minimum in the rotating shaft. Invoking the principle of minimum potential energy is a way to more easily derive the shaft energy related characteristics. The principle is used to analyze displacement and end points boundary conditions. Boundary conditions give prescription of displacements. The principle of virtual displacements and that of the minimum potential energy give the so-called stiffness (or displacement) method. The primary unknowns in that are the nodal displacements instead of the nodal forces. The strain-energy-density factor represents the strength of the elastic energy field in the vicinity of a crack-tip (with stress singularity) developed in the shaft. It was found that the energy which is a source of fluctuation in motion during shaft rotation was minimum when the total energy transferred to the shaft is minimum.

Keywords: Stiffness, Strain Energy, Minimum Potential Energy, Fatigue, Torsion

1. Introduction

A shaft is a rotating or stationary member, usually of circular cross-section, and may be subjected to bending, tension, compression, and fatigue loads acting singly or in combination. It is an important element of a machine and can support other rotating parts or transmit energy and power. Shafts are made of steel. When high strength is required, an alloy steel such as nickel, nickel-chromium or chromium-vanadium steel is used. The shaft originated from entire body of a long weapon composed of its pointed end and wearing portion, in the sixteenth century. This was extended generally to all bodies of long, cylindrical shape and an arrow (especially a long one, used with a long bow) in the fourteenth century. The mechanical sense, "long rotating rod for transmission of motive power and energy in a machine" and crank-shaft, shaft turned by a crank, appear to date from Roman times.

In addition to these, (Langston, 2013) stated that fluid was used as turbine property to turn the blades of a rotor attached to a shaft to perform useful work. Yongsheng *et al.* (2018) investigated the effects of fiber orientation, ratios of length over radius, ratios of radius over thickness on rotating composite shaft. They used a thin-walled composite shaft structure model, which included the transverse shear deformation of the shaft, rigid disks and the flexible bearings. This was then used to predict natural frequencies and dynamical stability. Based on the thin-walled composite beam theory, the displacement and strain fields of the shaft were obtained. The results compared with those in the literature. Shafts are extensively applied in rotating machinery in different engineering sectors. Many researchers have investigated the vibration characteristics of rotating shaft-disk systems. The shaft behaves like a spring (and so, is a mechanical energy storage device) as it exerts force when deformed. Sokolnikoff (2016) rigorously proved the principle of minimum potential energy. The J contour integral expressed the strain energy density at the crack tip by using a line integral.

Kolsky (2003) found that if a crack is planar and propagating horizontally, at velocities which do not involve a consideration of crack inertia, it can be assumed to have a constant value of the gravitational potential energy, and so, the energy transferred is the strain energy stored in the body. Boulenouar *et al.* (2016) evaluated the kinking angle at each crack increment length, as a function of the minimum strain energy density (MSED) around the crack tip. The results showed that in the framework of linear elastic fracture mechanics (LEFM), the minimum values of the density are reached at the points corresponding to the crack propagation direction. Yoon & Rao (1993) applied minimum normal principle, similar to the principle of minimum potential energy, for the synthesis of cam motion. This involved the use of piecewise cubic functions for representing the follower displacement. The result showed smaller peak acceleration and jerk. Ginsberg (2019) states that mechanical energy is dissipated in an under-damped free vibration. Energy is dissipated from one peak to the next. He determined the fraction of the mechanical energy dissipated in a cycle. In the absence of dissipation, the un-damped shaft was conservative. Bagci (2007) developed a three-dimensional flexural shaft element for elastic analyses of power transmission shafts and geared systems. Basic stresses are defined using the maximum energy of distortion theory. He determined strength reducing factors by using generalized expressions and redefined the dimensions for the desired factor of safety. Cook et al (2009) used a very simple spring system to show that the total potential energy has two parts: the strain energy and the potential of loads. The load was regarded as acting at its full value and does work moving through its displacement. The result showed that the load, in so doing, lost potential energy equal to the work done. It was concluded that the potential energy was the total external and internal work done in changing the configuration from the reference state to the displaced state. Neal-Sturgess (2017) developed a crack tip stress wave unloading model, estimated the energy released under the moving unloading wave front, and relates it to new surface generation. Sanford (2013) stated that failure theories can be deduced from energy-based arguments. The local stress field at the crack tip enters the formulation indirectly through its influence on the strain energy. In this study, the shaft dynamic loads are simulated for equilibrium, and shown to be affected by shaft properties such as stiffness (K) and inertia (J). Shigley & Mitchell (1993) stated that a shaft is a rotating or stationary member usually of circular cross-section, and may be subjected to bending, tension, compression, and fatigue loads acting singly or in combination. Bannantine *et al.* (2021) used unloading and reloading at a point in the plastic region of the stress-strain diagram to show that stress-strain response, demonstrated that the area under the hysteresis loops accounted for the energy involved. Reifsnider and Talug (2020) generated data dealing with various details of the process of damages that combine to produce a damage state which controls the state of strength of the degraded composite. The task of Hayes (2019) on factor of safety determination showed factor of safety separately for uncertainties that occur in the strength of the shaft and the uncertainties that may occur with load acting on it. This was done by producing a known load and noting that an estimated overload could be applied.

2. Materials and Methods

The selection of the material for this study is based on the attributes such as fatigue strength, and ductility [12].

2.1. Modelling

To fill the research gap of the existing modelling approach, the present study developed a unified modelling method for flexible shaft with general boundary conditions, by taking into consideration rotation-induced load. The composite shaft rotating along its longitudinal axis at a rate, θ_s, is shown in Figure 1. The assembly consists of a motor of power source connected by flexible shaft to the load.
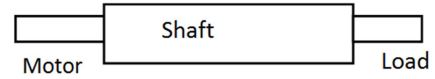

Figure 1. Shaft rotated by a motor.

In the configuration of the shaft, displacement, u = 0 before it was rotated.

When the shaft is in this static equilibrium position the potential energy was zero and the kinetic energy was a maximum. When deformed elastically by some system of applied loads, it always returned to its natural state when the loads are removed [8]. Then the strain energy density was positive. The shaft has geometrical characteristics as diameter, length, thickness, and radius of curvature. The structural modelling was based on the assumption that the shaft is characterized as a slender thin-walled elastic cylinder, satisfying d≪L, h≪d, h≪r, where L, h, r and d denote the length, thickness, radius of curvature and the maximum cross sectional dimension of the cylinder, respectively.

The torsional load is applied from the motor with specified power and speed capacities to be met [14]. There is concentration of deflections close to the region where the shaft and the bushings contact each order. Symbolically, the model assembly is represented by a mass-spring-damper, as shown in Figure 2.
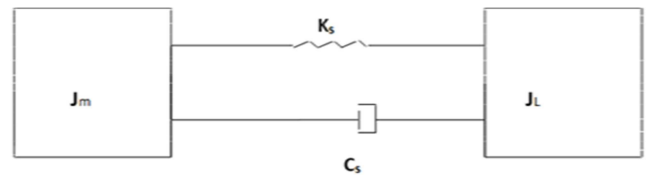

Figure 2. Mathematical Model.

Let θ_m, θ_s, θ_L be rotations of the motor, the shaft, and the load, respectively. Using standard procedures of analysis, the governing differential equations for the rotation give:

$$J_m\ddot{\theta} + C\,(\dot{\theta}_m - \dot{\theta}_L) + K\,(\theta_m - \theta_L) = T_m \qquad (1)$$

$$J_L\ddot{\theta} + C\,(\dot{\theta}_L - \dot{\theta}_m) + K\,(\theta_L - \theta_m) = -\,T_L \qquad (2)$$

where J_m and J_L are the polar area moments of inertia of the motor and of the load, respectively. It is given by $\int r^2 dA$, (r and A being shaft radius and area, respectively). The quantitative measure of J is the mass of the shaft. C is the damping coefficient. It represents friction (viscous, sliding, or any combination of the two). K is the stiffness of the shaft. It describes the magnitude of the force that bends the shaft a unit distance when applied [5]. In Equations (1) and (2), the functions are associated with physical behaviour for the axial strain, the bending curvatures, and the torsion twist rate [1]. They are used effectively for the analysis of tubular thin-walled structures. So, the shaft is a mechanical energy storage devise as it is spring-like and so has a spring constant, K. The over-dots indicate time differentiation. In this work, torque reactions are provided by Eqs. (1) and (2) ensuring that the shaft will work well. To maintain equilibrium, the bushing resists the torque [6]. To determine the rotating shaft's dynamical characteristics, this approach is carried out here to approximate the motion equations by a system of ordinary differential equations. Based on these approximate equations, the dynamical characteristics of the rotating shaft systems can then be calculated [13].

2.2. Energies Involved

The principle of minimum potential energy is such that out of all possible displacement fields that satisfy the geometric boundary conditions (i.e. the prescribed displacements), the one that also satisfies the equations of static equilibrium results in the minimum total potential energy of the shaft [4]. The sum of two different types of potential energy; that associated with the internal potential energy U_i (i.e. the strain energy) and that associated with the external potential energy U_e (i.e. from the external forces that act on the system), gives the total potential energy of the shaft,

$$\Pi = U_i + U_e \qquad (3)$$

It is the potential energy stored by the shaft when it is deformed through the distance u, and is defined by the average force times the deflection.

2.2.1. The Strain Energy
If the strain energy density is independent of the path followed in the strain space [3], the deformation of the shaft is hyper-elastic. In this project, the external work done on the elastic shaft in deforming it is transformed into strain or potential energy. The strain energies associated to this work (on rotating the shaft) are those of bending and shear. Some of the energies introduced into the shaft by the work done by displacements (deflections) in this operation, are not stored as strain energy, but are dissipated as the driving force for the internal process of crack growth [11]. The strain energy is the source of energy for crack propagation and is released as the crack extends. Since the strain energy decreased as the crack extended, this energy became available to the crack. The growth of crack results in surface energy. The surface energy is a well-defined measurable property of the material. Surface energy is a candidate receptor for the loss of strain energy

since new surfaces were created as the crack extends. The crack growth process continues as long as the rate of released strain energy extends the energy required to form a new surface. The work-energy theorem is used here to analyse rotation to find the work done on the system when it is rotated.

2.2.2. Mechanical Energy
This is dissipated in the under-damped free vibration. The non-conservative deformation process indicated that the loading history of an element of material in the neighbourhood of the deformation is different in the loading phase from the unloading phase so that a certain amount of energy is dissipated in the cyclic deformation process [2]. The mechanical energy E ≡ T (kinetic energy, the energy stored in the rotating shaft with moment of inertia J and angular velocity θ_s) + V (potential energy, corresponding to the peak values) is stored as potential energy. It is dissipated from one peak to the next (dissipated energy in a friction element with angular velocity). So, the fraction of the mechanical energy dissipated in a cycle can be determined [15]. In this study, with each damped cycle, a fraction of mechanical energy is lost to damping. In the absence of dissipation, the shaft is un-damped and conservative. The mechanical energy (T + V) is therefore constant. The shaft's inertia causes it to continue past the equilibrium position. Acting as a spring (and so spring constant, K) this property returns the shaft mass equilibrium by slowing it until it comes to rest at the maximum displacement. The kinetic energy is zero at that position and the potential energy is a maximum corresponding to maximum spring deformation [9]. The vibration continues periodically, with frequency because there is no damping to dissipate the mechanical energy. The damage evolution of fatigue hysteresis dissipated energy, and fatigue hysteresis modulus, fatigue peak strain, interface shear stress can be analysed [5].

For conservative force systems, the loss in the external potential energy during the loading process must be equal to the work done, W_e, on the system by the external forces, thus

$$- U_e = + W_e = - Fu \qquad (4)$$

where F is the force acting in full value, and u is the displacement. So, this represents the potential of loads as well.

$$\text{Eq. (3) becomes } \Pi = U_i + W_e \qquad (5)$$

This is the total internal and external work done in changing the configuration from the reference state of u = 0 to the displaced state u ≠ 0. Since the total potential energy, Π is afunction of functions (the strain and displacement functions), it is a functional. In order to minimize Π, we insist that the first variation of the total potential energy be zero, that is,

$$\delta\Pi = \delta U_i + -\delta W_e = 0 \qquad (6)$$

or

$$\delta U_i = \delta W_e \qquad (7)$$

where δU_i is the first variation in the strain energy (as a result of the variation in the strain). With K as the stiffness of the shaft,

$$U_i = \frac{1}{2}KD^2 \qquad (8)$$

Equation (3) becomes

$$II = \frac{1}{2}Ku^2 - Fu \qquad (9)$$

The rotational potential energy U_i is stored in a rotational shaft with spring constant K and deflection u [7]. The equilibrium configuration, u_{eq} is found from the stationary value of II.

$$dII = (ku_{eq} - F)du = 0 \rightarrow u_{eq} = \frac{F}{K} \qquad (10)$$

Displacement fields satisfying the equations of static equilibrium, Eqs. (10), result in the minimum total potential energy of the shaft.

2.3. Simulation

Simulation is accomplished by applying a standard maximum deflection of 0.2 mm at the middle of the shaft, and then varied. The distance between bearings can also influence lateral deflection. The critical sections of the shaft in this project (the sections with abrupt change in cross-section), Figure 1, were considered. They are subjected to the motor torque, the load torque, and flexing action. The geometry of the shaft influences the flexural endurance. The product of its elastic modulus, E and the planar moment of inertia I, i.e. EI, gives the shaft its flexural rigidity. Bubbles, voids, and contamination are eliminated from the shaft expected to perform in this demanding flex applications. Each of these defects can become the nucleus of failure (due to crack action) after the part has been subjected to flexing action. Fatigue life analysis model based on classical fracture mechanics (using APDL, ANSYS Parametric Design Language) code gives estimate of remaining fatigue life [10]. The flexural moment is negligible as bending fatigue strength is not affected by the existence of torsional mean stress until the torsional yield stress is exceeded by about 50% (Sines and Waisman, 1959). In this work, application of a factor of safety helped the shaft to sustain the minimum energy level.

2.4. Energy Method for Force-Displacement Relations and Boundary Conditions

In this work, the shaft is modelled to have specific force-displacement relations and a standard varying deflection. For example, it exerts a force when deformed. Boundary conditions are constraints necessary for the solution of a boundary value problem on whose boundary, a set of conditions is known. Equating internal work to external work,

$$\frac{d}{du}II_p = \frac{d}{du}[-Fu + \frac{AE}{2L}u^2] = 0 \qquad (11)$$

$$[-F + \frac{AE}{L}u] = 0 \rightarrow P = \frac{AE}{L}u \qquad (12)$$

Equations (11) and (12) represent the force- displacement relations of the rotated shaft in equilibrium.

In this study, displacement in the element is defined as u_i, and u_j, the possible displacement fields that satisfy the geometric boundary conditions. Assuming

$$u = a_1 + a_2x$$

$$u = (1 - \frac{x}{L})u_i + (\frac{x}{L})u_j \qquad (13)$$

where x and L define the boundary conditions of the shaft length. Knowledge of deformations is specified in terms of strains, that is, the relative change in the size and shape of the body. Poisson ratio gives the ratio of transverse strain to axial strain. The deformation resulted from stress. One reason for this is that the steel is used within its design limit, i.e. proportional limit (before yield). In that region, axial strain is proportional to lateral strain. In compression, the deformation of the steel material stressed along (in the direction of) one axis produced a deformation of the material along the other axis in three dimensions. Summing strain energy at a point for the element,

$$u_i = \int_0^L \frac{AE}{2}(\frac{du}{dx})^2 dx \qquad (14)$$

Substituting $u = (1 - \frac{x}{L})u_i + (\frac{x}{L})u_j$ into u_i and integrating:

$$u_i = \frac{AE}{2L}[u_i^2 - 2u_iu_j + u_j^2]$$

$$u_i = \frac{AE}{2L}\begin{bmatrix} 1 & -1 \\ -1 & 1 \end{bmatrix}\begin{Bmatrix} u_i \\ u_j \end{Bmatrix} = \begin{Bmatrix} P_i \\ P_j \end{Bmatrix} \qquad (15)$$

This is strain energy in terms of stiffness (or displacement) method. The solution is based on prescribed displacement fields. Since the stiffness matrix, Equation (15), is correct, the geometric boundary condition is satisfied. Satisfying the condition establishes stable equilibrium and minimum potential energy [6].
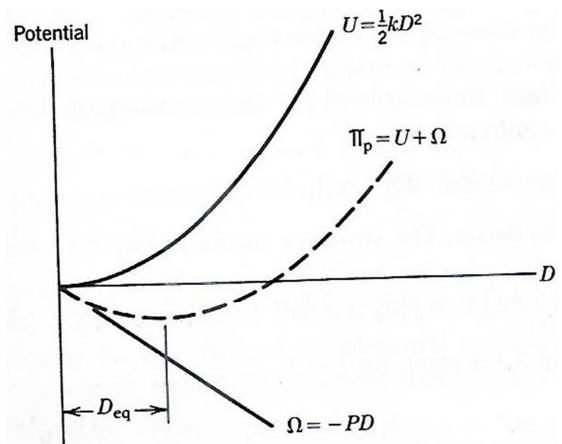

Figure 3. Minimum potential energy, from Cook et al. (2009).

The principle of minimum potential energy requires that the total potential energy, II be a minimum for stable equilibrium.

In Figure 3, Cook et al. plotted minimum potential energy with dotted lines. Minimum potential energy falls below the

displacement axis.

3. Results and Discussion

The energy transformed via the shaft into kinetic energy is, in turn, converted into force (KD) on the load mounted on the shaft. The ability of the motor to generate a rotary motion on the shaft that transmits kinetic energy to drive the load made the shaft suitable for this operation.

In the dynamics study, the rotating shaft was represented as a thin-walled structure of circular cross-section. Consistent with the study the effect of increase in stiffness and tension, the high stiffness of the steel initially resulted in any effect from torsional vibration to be negligible. The stiff material has a higher elastic modulus and deflects the effect of vibrational waves better. However, the stiffness decreased as deflection increased.

3.1. Torque Reaction Provided by the Model

The equilibrium conditions are satisfied by the following dynamic equations:

$$J_m\ddot{\theta} + C\,(\dot{\theta}_m - \dot{\theta}_L) + K\,(\theta_m - \theta_L) = T_m$$

$$J_L\ddot{\theta} + C\,(\dot{\theta}_L - \dot{\theta}_m) + K\,(\theta_L - \theta_m) = -T_L$$

3.2. Resultant Forces

In solids, the work done by external loads is stored as recoverable strain energy. For deformable elastic bodies under loads, the strain energy stored in the body per unit volume is then defined clearly.

Table 1. *External Potential Energy Related to Displacement.*

External Potential Energy U_e (- Fu)	Displa-cementu	Force P (Ku)
- 0.12	0.02	5.81
- 0.23	0.04	11.62
- 1.05	0.06	17.43
- 1.86	0.08	23.24
- 2.90	0.10	29.04

In Table 1, as displacement increased, external potential energy decreased. This is due to the fact that the load F (the bearing force) is always acting at full value. In moving through the displacement u, it does work in the amount Fu. In so doing it loses potential of equal amount, and that means negative Fu (or – Fu), as shown in Table 1.

Table 2. *Displacement Relation to Internal Energy ($\frac{1}{2}kD^2$).*

Displacementu (mm)	Strain EnergyU_i
0.02	0.06
0.04	0.23
0.06	0.52
0.08	0.93
0.10	1.45

Table 2 shows that displacement also increases with increasing internal energy.

Table 3. *Total Potential Energy and Displacement.*

Total PotentialEnergyΠ_p $\times10^3$	Displacementu
0.00	0.00
- 0.06	0.02
0.00	0.04
0.53	0.06
0.93	0.08
1.45	0.10

In table 3, displacement increased from 0.00 to 0.02 with decreasing total potential energy. After, that total potential energy increased with increasing displacement. At 0.04 displacement, the total potential energy came to zero and continued to increase to positive values. Therefore, the minimum potential energy of -0.6 resulted at 0.02 displacement. The minimum potential energy results obtained in this work correlates with those of Cook et al. (2009), as shown in Figure 3.

4. Conclusion

From the present analysis, the following main conclusions can be obtained:

1) The total potential energy of the shaft has two parts, the strain energy and the external potential energy.
2) The displacement at which the total potential energy is minimum was the equilibrium displacement (i.e. 0.02). At this event, the equilibrium state is stable.

This paper deals with the structural modelling and dynamical analysis of a rotating shaft. Simulations of the effects of the various parameters including geometric dimension and the transverse shear deformation on frequencies and critical rotating speeds were performed. The analytical model developed in this study can be used to highlight the dynamic behaviour of a rotating shaft system. The present model can further be extended to incorporate the effects of internal damping of a shaft for evaluating the dynamic instabilities due to internal damping. This has been an improvement.

References

[1] Bagci, C. (2007). Computer-Aided fatigue Design of Power Transmission Shafts Using Tree-Dimensional Finite Shaft Element and Updated Mean Stress Diagram. *Journal of Mechanical Design 12 (79),* 10-12.

[2] Bannantine, J., Comer, J., & Handrock, J. (2021). Fundamentals of Metal Fatigue Analysis. Eaglewood Cliffs, NJ: Prentice.

[3] Boulenouar, A., Benseddiq, M., Mohamed, M., Benamara, N., & Mazari, M. (2016). A strain energy density theory for mixed mode crackpropagation. *Journal of Theoreticaland Applied Mechanics, 54* (4), 17–31.

[4] Cook, R., Malkus, D., & Plesha, M. (2009). *Concepts and Applications of Finite Element Analysis.* New York: John Wiley.

[5] Ginsberg, J. (2019). *Mechanical andStructural Vibrations Theory and Applications.* New York: John Wiley.

[6] Hayes, J. (2019). *Fatigue Analysis and Fail-Safe Design of Vehicle Structures,* (2nd. Ed.) Cincinnati, Ohio: E. F. Bruhn Educational.

[7] Kolsky, H. (2003). *Stress Waves in Solids*. New York: Dover.

[8] Langston, L. (2013). *The Adaptable Gas Turbine.* [e-book]. Retrieved fromhttp://books.google.co.nz. 23/09/2022

[9] Neal-Sturgess, C. (2017). (p. 1). A direct derivation of the Griffith – Irwin relationship using a crack tip unloading stress wave model. Retrieved from http://www.google.com.Fatigue.

[10] Reifsnider, K., & Talug, A. (2020). Analysis of Fatigue Damage in Composite Laminates. *International Journal of Fatigue 2* (1), 456-500.

[11] Sanford, R. (2013). *Principles of Fracture Mechanics.* Upper Saddle River: Prentice Hall.

[12] Shigley, J., & Mitchell, L. (1993): *Mechanical engineering design.* (6th. Ed.), New York: McGraw-Hill.

[13] Sokolnikoff, I. (2016). *Mathematical theory of elasticity*, (2nd Ed.). New York: McGraw-Hill.

[14] Yongsheng, R., Qiyi, D., & Xingqi, Z. (2018). Modeling and dynamicanalysis of rotating composite shaft. *Journal of Vibroengineering* 15 (4), 1790-1806.

[15] Yoon, K., & Rao, S. (1993). Cam motion synthesis using cubic splines. *Journal of Mechanical Design 8 (3),* 15-41.